Journal of Applied Polymer Science

Oxoacetohydrazide-functionalized cellulose with enhanced adsorption performance

Shiyong Xiao,[1] Qizhong Xiong,[1] Hongjian Zhou,[1] Yunxia Zhang,[1] Guozhong Wang,[1] Haimin Zhang,[1] Huijun Zhao[1,2]

[1]Key Laboratory of Materials Physics, Centre for Environmental and Energy Nanomaterials, Anhui Key Laboratory of Nanomaterials and Nanotechnology, Institute of Solid State Physics, Chinese Academy of Sciences, P.O. Box 1129, Hefei 230031, People's Republic of China

[2]Centre for Clean Environment and Energy, Gold Coast Campus, Griffith University, Queensland, 4222, Australia

Correspondence to: H. Zhao (E-mail: h.zhao@griffith.edu.au) and Q. Xiong (E-mail: qzxiong@issp.ac.cn)

ABSTRACT: A simple and environmental friendly oxoacetohydrazide functionalization method is developed to convert the straw cellulose into high performance adsorbents for effective Pb(II) removal. The adsorption experimental results demonstrated that the resultant oxoacetohydrazide-modified cellulose (OMC) possesses a dramatically improved Pb(II) adsorption capacity (82.9 mg/g), which is over six times of that for the unmodified celluloses (13.6 mg/g). The mechanistic studies confirm that the markedly enhanced Pb(II) adsorption capability of OMC can be attributed to the formation of N-Pb-N bonds resulting from the strong chelating interactions of Pb(II) with oxoacetohydrazide. Also, the OMC shows an excellent reusability, capable of retain 95% of its original Pb(II) adsorption capacity after three consecutive adsorption cycles. The findings of this work pave a way to transform the agricultural byproducts into high performance functional materials. © 2015 Wiley Periodicals, Inc. J. Appl. Polym. Sci. **2016**, *133*, 42950.

KEYWORDS: adsorption; cellulose and other wood products; functionalization of polymers

Received 30 July 2015; accepted 15 September 2015
DOI: 10.1002/app.42950

INTRODUCTION

Cellulose is the most abundant renewable natural polysaccharide that exists as a primary constituent of cellulosic biomass such as plants. Due to its virtually unlimited availability, renewability, non-toxicity and cheap to obtain, the cellulose has been widely utilized in paper, food, medicine, energy, textile industries, and environmental remediation applications.[1–7] In contrast to starch, cellulose is a natural polymer of β-D-glucose with -CH_2OH groups alternating above and below the planar of the cellulose molecule to form long, non-branched chains with pyranose and hydroxyl groups.[8] These functional groups together with the high porosity and surface area make the cellulose a promising adsorbent for pollutants removal applications.[9,10] However, the unmodified natural celluloses often show low adsorption capacity and poor selectivity toward heavy metal ions due to the intra- and intermolecular hydrogen bonding in natural celluloses that hinder the adsorptivity of hydroxyl and ether groups.

In order to improve the adsorption performance, an extensive effort has been made to functionalize the natural cellulose by introducing new functional groups via various modification approaches, including acidification action,[11] etherification,[12] esterification,[13] amination,[14,15] grafting polymerization,[16] and cross-linking.[17] Among these functionalization approaches, the introduction of amide or amino groups to original cellulose structure has demonstrated to be an effective means to improve the performance of heavy metal adsorption via the enhanced complexation with metal ions. Aoki and co-workers reported an amino modified cellulose adsorbent for aquatic heavy metal removal, with saturated adsorption capacities of 22 mg/g, 28 mg/g and 8 mg/g, for Cu(II), Pb(II) and Ni(II), respectively.[18] Zhao et al. prepared the amide modified cellulose pulps by grafting copolymerization under microwave irradiation, the resultant adsorbent possesses a saturated adsorption capacity of 49.6 mg/g for Cu(II).[19] Despite the demonstrated adsorption performance improvement for some heavy metals, the extent of the enhancement is limited, mainly because only single functional group (amino or amide) is introduced.

Recently, a number of groups proposed a double or multiple functional groups modification strategy to improve the adsorption performance of other types of adsorbents. Monier et al. employed a three-step chemical modification route (graft copolymerization, hydrazinolysis and amidation) to graft the hydrazide onto the surface of wools.[20] The hydrazide-modified

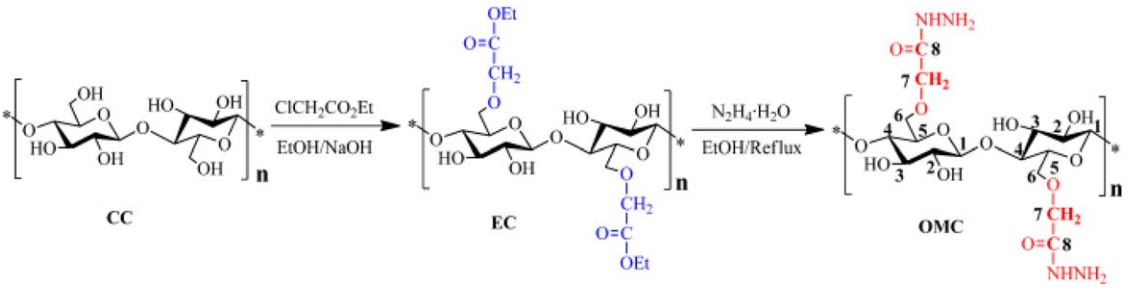

Scheme 1. Synthetic route of OMC. [Color figure can be viewed in the online issue, which is available at wileyonlinelibrary.com.]

wools exhibit a significantly improved adsorption capacity and superior selectivity toward mercury ions. Wang et al. prepared hydrazide piperidinepolythiophene derivatives via a synthetic route of substitution, hydrazinolysis, and oxidative polymerization.[21] The resultant adsorbents show high adsorption capacity and selectivity to the divalent copper and mercury ions. Although these reported modification approaches may not be directly adoptable for modification of cellulose based adsorbents, the demonstrated benefits of such functional groups motivate us to develop an effective modification method capable of introducing new adsorption functional groups into cellulose to enhance the adsorption capacity of heavy metals for cellulose-based adsorbents.

The oxoacetohydrazide contains bi-functional groups of amide and amino, both have strong tendency to form complexes with Pb(II).[22,23] In this work, we propose and experimentally validate a simple functionalization approach through etherification and hydrazinolysis of cellulose using environmentally friendly ethanol solvent under alkaline conditions to obtain the oxoacetohydrazide-modified cellulose (OMC). The adsorption performance of the resultant OMC for selective removal of aquatic Pb(II) is systematically investigated. The synergetic electron redistribution in the oxoacetohydrazide chemically linked on C-6 of cellulose structure (Scheme 1) could liberate the lone-electron pair of the amide N to enhance oxoacetohydrazide's chelating ability toward heavy metal ions. The mechanistic aspects of the enhanced adsorption capability of OMC are investigated. The selection of cellulose extracted from the corn straws is because the straws are common agricultural by-products, plentiful and easier to collect for centralized treatment. Currently, other than small portions being effectively utilized, the vast majority of straws are consumed via onsite burning and landfill, causing serious environmental issues. We hope that the findings presented in this work would pave a way for development of cellulose-based high performance adsorbents from agricultural by-products.

EXPERIMENTAL

Materials and Reagents

The cellulose was obtained from corn straw by chemical extraction.[24] Ethyl chloroacetate was supplied by Aladdin Industrial Corporation (Shanghai) and hydrazine solution (80 wt %) was purchased from Sigma-Aldrich Co. Ltd., lead nitrate was obtained from Tianjin Guangfu Fine Chemical Research Institute. Nitric acid, sodium hydroxide, ethyl alcohol and other chemicals were purchased from Sinopharm Chemical Co. Ltd. (China). The deionized water was produced using a Millpore Milli-Q grade, with a resistivity of 18.2 MΩ/cm. All other chemicals used in this study were of analytical grade and used without further purification.

Synthesis of Corn Straw Cellulose and OMC

The corn straw cellulose (CC) was obtained by a reported extraction technique.[24] A typical synthesis process is as follows: 10 mg of corn straw was firstly refluxed to dewax in a 250 mL flask with a mixture of 60 mL of benzene and 120 mL of ethanol for 6 h. After that, the lignin in the sample was removed using glacial acetic acid acidified sodium chlorite solution (pH ≈ 3.0) at 75°C for 1 h; the process was repeated five times to obtain white extractive. The extractive was then treated over night with 2.0 wt % potassium hydroxide at room temperature to remove hemicelluloses, residual starch, and pectin. The extractive was subsequently treated with an acetic acid acidified sodium chlorite solution (pH ≈ 3.0), and then treated with 6.0 wt % potassium hydroxide at 80°C for 2 h. Highly purified CC was obtained by further treating the extractive with 1.0 wt % hydrochloric acid solution at 80°C for 2 h and thoroughly washing them with distilled water. The final CC product was freeze-dried and stored for further use.

The as-synthesized CC was used as starting material for further functionalization. Scheme 1 schematically illustrates the synthesis process of OMC. Briefly, the obtained CC (10 g) was firstly dispersed in 60 mL of ethyl alcohol solvent containing 4.8 mg of NaOH (0.12 mmol) under constant stirring for 1 h. Ethyl chloroacetate (15 μL, 0.14 mmol) was then added dropwise to the above solution under gentle stirring. The solution mixture was subsequently refluxed at 85°C in an oil bath for 6 h to complete the etherification reactions. After etherification, the resultant mixture was washed successively with deionized water and ethanol. The solvent was removed by vacuum drying. The etherified cellulose (EC) was subjected to hydrazinolysis treatment by refluxing in an ethanol solution (60 mL) containing hydrazine monohydrate (25 μL, 0.52 mmol) for 24 h. Finally, the resultant white precipitates (OMC) were collected and washed with deionized water and ethanol, then dried in a vacuum oven at 60°C for 6 h. The dried OMC was stored for further characterization and adsorption experiments.

Characterization

The size and morphology of the as-synthesized samples were characterized using a field emission scanning electron microscope (FESEM, Sirion 200 FEI) with an accelerating voltage of 10.0 kV. The Fourier transform infrared (FT-IR) spectra were

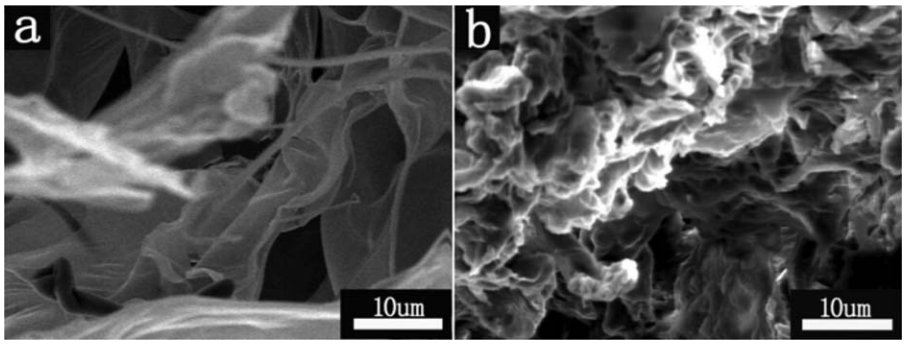

Figure 1. FESEM images of (a) CC and (b) OMC.

measured on a Nicolet-Nexus FT-IR spectrometer with the KBr pellet technique ranging from 400 cm^{-1} to 4000 cm^{-1} at room temperature. The pH values were monitored on a Mettler Toledo pH meter (FG2/EL2). The elemental analysis (EA) of the samples was performed by VarioEL(III) elemental analyzer from Germany. The Solid Carbon Nuclear Magnetic Resonance (^{13}C-NMR) spectra were performed on a Bruker AV III 400 WB spectrometer operating at a ^{13}C resonance frequency of 100.6 MHz. The valence states of OMC or Pb-OMC and mechanistic model of adsorption process were analyzed by X-ray photoelectron spectroscopy (XPS, Thermo ESCALAB 250) using monochromatized Al Ka(hv=1486.6 eV, power=150 W) X-ray beams as the excitation source. Binding energies were calibrated relative to the C 1s peak at 284.6 eV. The concentration of Pb(II) was performed with an Inductively Coupled Plasma Optical Emission Spectroscopy (ICP-OES) from Thermo Fisher (Thermo iCAP 6300). A shaking thermostatic bath (SHZ-B, China) was used for oscillating the solution.

Adsorption Experiments

Pb(II) stock solution (1000 mg/L) was prepared by dissolving an appropriate amount of $Pb(NO_3)_2$ in deionized water. The concentrations of Pb(II) were confirmed by ICP-OES. For the isothermal adsorption experiments, the conical flasks with the absorbents and Pb(II) solution were placed in a shaker (300 rpm) for a fixed time, then followed by filtration to remove the adsorbent. Samples were withdrawn when adsorption reaches equilibrium and centrifuged. The amount of adsorbed Pb(II) per unit mass of the adsorbent was calculated by:

$$Q = \frac{C_0 - C_e}{m} \cdot V \quad (1)$$

where Q (mg/g) is the equilibrium adsorption capacity; C_0 and C_e (mg/L) are the initial and equilibrium concentrations of Pb(II) in solution, respectively; V (L) is the volume of solution and m (g) is the mass of adsorbents. And series of experiments were conducted to determine the effects of solution pH and the temperature on adsorption capacity. Effect of initial solution pH on adsorption was tested at various pH values ranging from 2 to 6. Solution pH was adjusted with 0.1*M* HCl or NaOH solutions.

The OMC recycle experiments use the same procedure as described above. Between each consecutive recycle, the OMC adsorbents were regenerated by immersing in a 1*M* HCl solution (100 mL) and shaking at 300 rpm for 1 h using a shaking thermostatic bath at 50°C.

RESULTS AND DISCUSSION

Characteristics of OMC

The obtained CC [Figure 1(a)] from corn straws was subjected to the etherification and hydrazinolysis to obtain OMC with amide and amino groups at the C-6 on cellulose (Scheme 1). Figure 1(b) shows a typical FESEM image of the resultant OMC formed by randomly packed nanosheets. Comparing to the

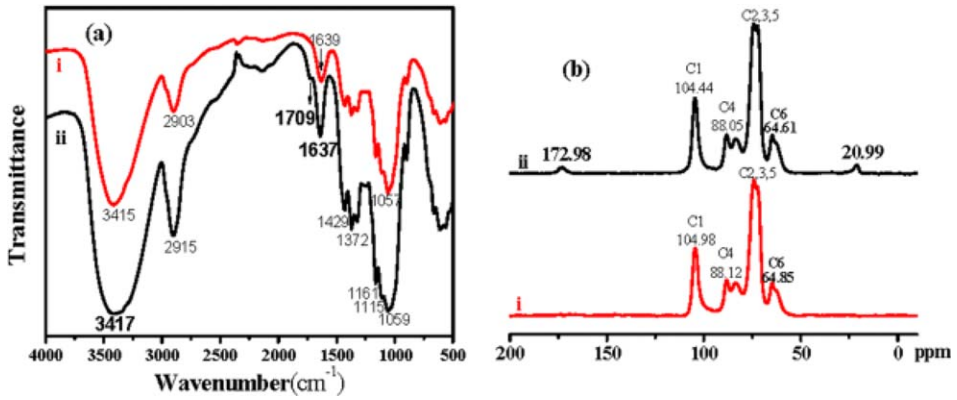

Figure 2. (a) FT-IR spectra of CC (curve i) and OMC (curve ii) and (b)^{13}C-NMR spectraof CC (curve i) and OMC (curve ii). [Color figure can be viewed in the online issue, which is available at wileyonlinelibrary.com.]

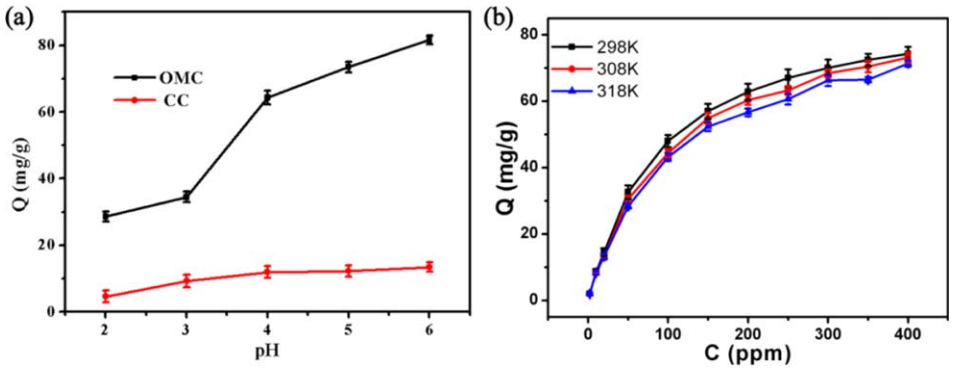

Figure 3. (a) Effect of pH on Pb(II) adsorption on OMC and CC; (b) Effect of temperature on Pb(II) adsorption on OMC. [Color figure can be viewed in the online issue, which is available at wileyonlinelibrary.com.]

unmodified CC, OMC possesses a rougher surface, which could be beneficial for interaction with heavy metal ions.

The FT-IR spectra of OMC [Figure 2(a)] confirm the presence of a new absorption band cantered at 1709 cm^{-1} that can be assigned to —C═O.[25] The broad absorption band peaked at 3415 cm^{-1} could be due to the stretching vibration of —OH and/or —NH groups. The absorption band around 1637 cm^{-1} can be attributed to the N—H and/or C—H bending vibrations.[26] These FT-IR evidences suggest that oxoacetohydrazide has been successfully introduced to OMC.

NMR is one of the most effective means for precise structural analysis. Figure 2(b) shows the ^{13}C-NMR spectra of CC and OMC. The NMR spectrum between δ 64.61 and δ 104.98 ppm represents the structural characteristics of glucose unit in cellulose.[27,28] Very similar NMR spectra obtained from both samples within this chemical shift range indicate that the oxoacetohydrazide modification has very minor effect on the six glucose carbons in the cellulose structures. However, the spectrum obtained from OMC reveals two new chemical shift peaks at δ 20.99 and 172.98 ppm that can be, respectively, assigned to methylene (C-7) and hydrazide (C-8) carbons (Scheme 1), confirming oxoacetohydrazide has been successfully introduced.[29] Also, the signal for C-6 is shifted slightly from δ 64.85 to δ 64.61 ppm due to the chemical environmental changes introduced by oxoacetohydrazide modification.

The elemental analysis shows that the as-synthesized OMC contains 37.47% and 0.45% of C and N, respectively. Assuming all

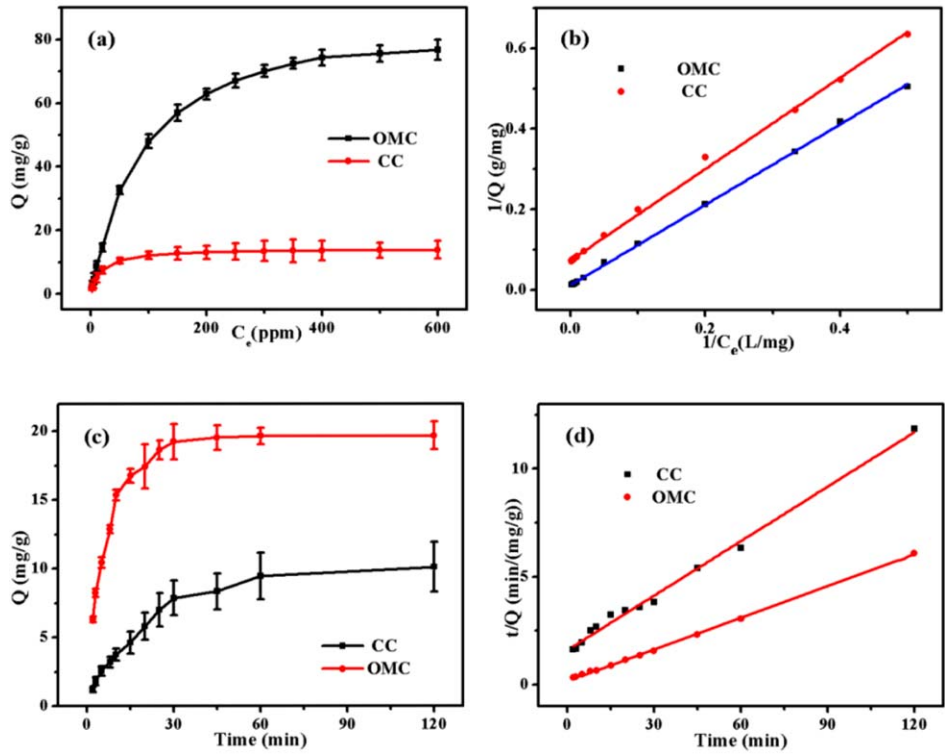

Figure 4. (a) Pb(II) adsorption isotherms, (b) Langmuir model plots, (c) Dynamic adsorption of Pb(II), (d) The pseudo-second-order kinetics model plots. [Color figure can be viewed in the online issue, which is available at wileyonlinelibrary.com.]

Table I. Langmuir Isotherm Models Constants

	Langmuir isotherm parameters		
Adsorbent	Q_m (mg/g)	K_L (L/mg)	R^2
OMC	82.9	0.012	0.9996
CC	13.6	0.065	0.9976

determined N contents in OMC are contributed by the modified oxoacetohydrazide, a 0.45% of *N* should correspond to ~4% of C-6 in the resultant OMC being modified with oxoacetohydrazide. Considering the majority of modifications should occur on the cellulose surface, this result implies that the oxoacetohydrazide modified surface C-6 should be higher than 4%.

ADSORPTION

The Effects of pH and Temperature

The pH is an important parameter affecting metal-chelate formation. The effect of pH on the adsorption of Pb(II) was investigated within pH 2–6 [Figure 3(a)]. In this study, only pH≤6 was investigated because of hydrolysis of metal ions at higher pH. The results clearly reveal that the Pb(II) adsorption capacity of OMC are higher than that of CC. The highest adsorption capacity was observed at pH 6.0, similar to those previous reported adsorption behaviors of other adsorbents.[30,31] For both CC and OMC, an increase in pH leads to an increased Pb(II) adsorption capacity. For OMC, most of the functional groups such as —NH— and —OH were protonated and presented in the positively charged form at low pH, which reduce the number of active binding sites. Also, the electrostatic repulsion between Pb(II) and the positively charged functional groups might negatively affecting the adsorption of Pb(II) onto the surface of the adsorbents. Therefore, the adsorption of Pb(II) in acidic solution was unfavorable. As the pH value increased, the protonated —NH— and —OH groups are gradually deprotonated and more active binding sites available, favorable for the formation of the complex with Pb(II). These could be the reasons for the observed sharp increase in Pb(II) adsorption capacity when pH was increased from 3 to 4.

The effect of temperature on Pb(II) adsorption onto OMC was investigated at pH=6 [Figure 3(b)]. Although a decreased tread in adsorption capacity is clearly visible with the increased temperature, the changes in adsorption capacities are small, suggest the adsorption is likely via relatively strong chemisorption processes rather than weak physisorption processes.

Adsorption Isotherm. The adsorption behavior of OMC and CC were investigated. Figure 4(a) shows the adsorption isotherms of Pb(II) at 25°C and pH 6.0. For the two cases investigated, an increase in the concentration of Pb(II) leads to a rapidly increased equilibrium adsorption amount of Pb(II) in the low concentration range and gradually saturates in the high concentration range. For OMC, near 100% removal efficiencies can be achieved for original solutions containing less than 10 ppm of Pb(II). For original solutions containing over 20 ppm of Pb(II), approximately 90% removal efficiencies can still be maintained. In contrast, for CC adsorbent, only ~50% removal efficiencies can be achieved for original solutions containing less than 10 ppm of Pb(II), while for original solution containing over 20 ppm of Pb(II), nearly 80% of Pb(II) are still retained in solution.

The Langmuir model [eq. (2)] is only valid monolayer adsorption.[32]

$$\frac{1}{Q}=\frac{1}{Q_m}+\frac{1}{K_L Q_m C_e} \tag{2}$$

where Q and Q_m are the equilibrium and maximum adsorption amounts, respectively; C_e is the equilibrium concentration and K_L is the Langmuir adsorption constant. A linear relationships between $1/Q$ and $1/C_e$ confirms that the measured Pb(II) adsorption isotherms for both OMC and CC can be well fitted to the Langmuir model [Figure 4(b)]. K_L and Q_m can be determined from the slope and intercept of the curve, respectively (Table I). The adsorption capacities of OMC and CC calculated from Langmuir model are 82.9 mg/g and 13.6 mg/g, respectively. These results indicate that the adsorption capacity of OMC is more than five times of that for CC, demonstrating the effectiveness of the oxoacetohydrazide modification.

Kinetics Study. The adsorption kinetic behavior was also investigated. All adsorption kinetic experiments were performed in a solution containing 10 ppm Pb(II)at pH 6.0 and the adsorption amounts were determined at predetermined time intervals. It was found that the adsorption reaches the equilibrium status within 30 and 60 min for OMC and CC, respectively. Under the equilibrium status, 95% and 50% of Pb(II) in the adsorption solution can be removed by OMC and CC, respectively. These results confirm the superior adsorption performance of OMC over CC, further demonstrating the effectiveness of oxoacetohydrazide modification. The Figure 4(c) illustrated the adsorption of Pb(II) on OMC and CC from aqueous solution as a function of contact time. The obtained adsorption kinetic data were analyzed using pseudo-first-order[33] and pseudo-second-order kinetic models [see eqs. (3) and (4)].[34]

Table II. The Two Kinetic Model Parameters for Pb(II) Ions Adsorbed onto Adsorbents

	Pseudo-first-order model				Pseudo-second-order model		
Adsorbent	Q_{exp}[a] (mg/g)	Q_{1e} (mg/g)	K_1 (min)	R^2	Q_{2e} (mg/g)	K_2 (g mg/min)	R^2
OMC	19.8	16.7	0.033	0.664	20.5	0.0076	0.999
CC	11	8.8	0.021	0.943	11.9	0.0044	0.993

[a] The experiment data.

Table III. Comparison of the Maximal Adsorption Capacities of Different Functionalization Modified Cellulose Adsorbents toward Pb(II) Ions

Adsorbents	Q_m (mg/g)	pH	Initial Pb(II) Conc. (ppm)	Ref.
Cellulose/chitin beads	68.4	4.0	280	35
Thiol-modified cellulose composite membranes	137.7	5.5	50	31
Diethylenetriamine bacterial cellulose	31.4	4.5	100	36
Ethylenediamine-modified cellulose	50.0	6.0	200	37
6-Deoxy-6-mercaptocellulose derivatives	28.0	5.0	4144	18
Triethlenetetramine-modified cellulose	147.1	5.7	320	15
Collagen/cellulose hydrogel beads	454.2	4.2	932	38
Amidoximated bacterial cellulose	67.0	5.0	200	39
Carboxymethylated bacterial cellulose	60.4	4.5	100	40
OMC	82.9	6.0	100	This study

$$\log(Q_e - Q) = \log Q_e - K_1 t \quad (3)$$

$$\frac{t}{Q} = \frac{1}{K_2 Q_e^2} + \frac{1}{Q_e} \quad (4)$$

where Q and Q_e represent the amount of contaminant Pb(II) adsorbed on adsorbent (mg g^{-1}) at any time and at equilibrium t (min), respectively, and K_1 (min^{-1}) is the kinetic rate constant for the pseudo-first-order model. And K_2 (g mg/min) is the rate constant of pseudo-second-order adsorption. The slope and intercept of the plot of t/Q versus are used to calculated K_2 and Q_e [Figure 4(d)], and the corresponding kinetic parameters from this model are listed in Table II. Figure 4(d) shows the fitting of adsorption kinetic data to the pseudo-second-order kinetic model with a near unity correlation coefficient ($R^2 > 0.99$), indicating the adsorption kinetic data obtained from both OMC and CC can be well fitted to pseudo-second-order kinetic model. This indicates the chemical adsorption was likely to be the dominant adsorption process.[34] Table II shows the key kinetic parameters and the correlation coefficients to pseudo-first-order and pseudo-second-order kinetic models. The obtained correlation coefficients indicate that the adsorption kinetic data of OMC cannot well fitted to the pseudo-first-order kinetic model ($R^2 = 0.664$).

To further demonstrate OMC's adsorption performance toward Pb(II), we compared the maximal adsorption capacities of different functionalization modified cellulose adsorbents in literatures (Table III). As shown in Table III, all functionalized cellulose adsorbents exhibited the maximal adsorption capacity toward Pb(II) ions within solution pH 4.0–6.0 (Table III). Moreover, the OMC in this work demonstrated high adsorption performance toward Pb(II) ions. Although several studies showed better adsorption performance than OMC in this work, the initial Pb(II) ion concentrations in their studies are

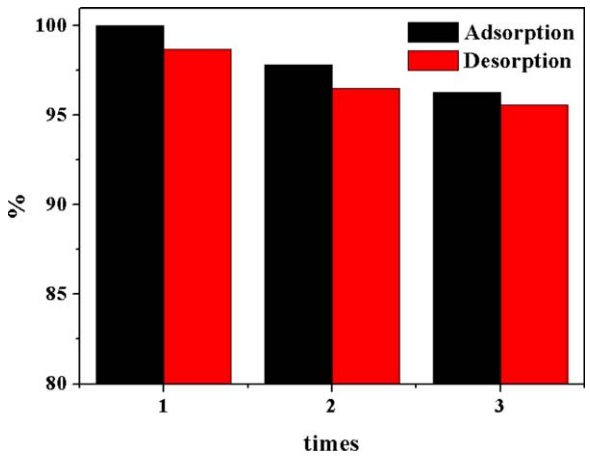

Figure 5. Pb(II) adsorption and desorption efficiencies of OMC during three consecutive cycles. [Color figure can be viewed in the online issue, which is available at wileyonlinelibrary.com.]

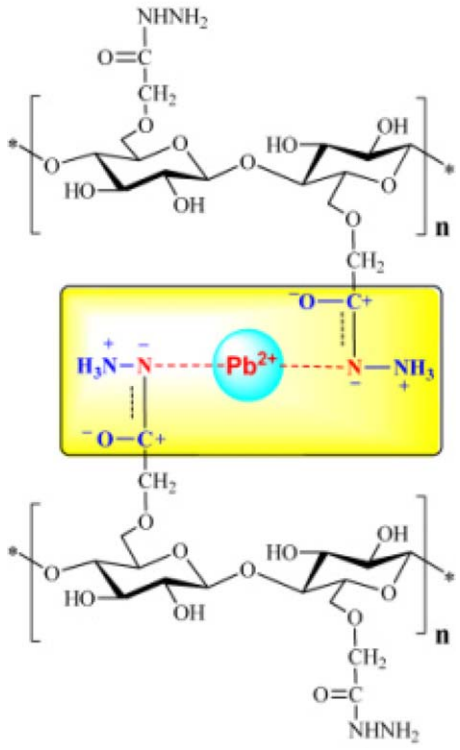

Scheme 2. Proposed Pb(II)adsorption mechanism on OMC. [Color figure can be viewed in the online issue, which is available at wileyonlinelibrary.com.]

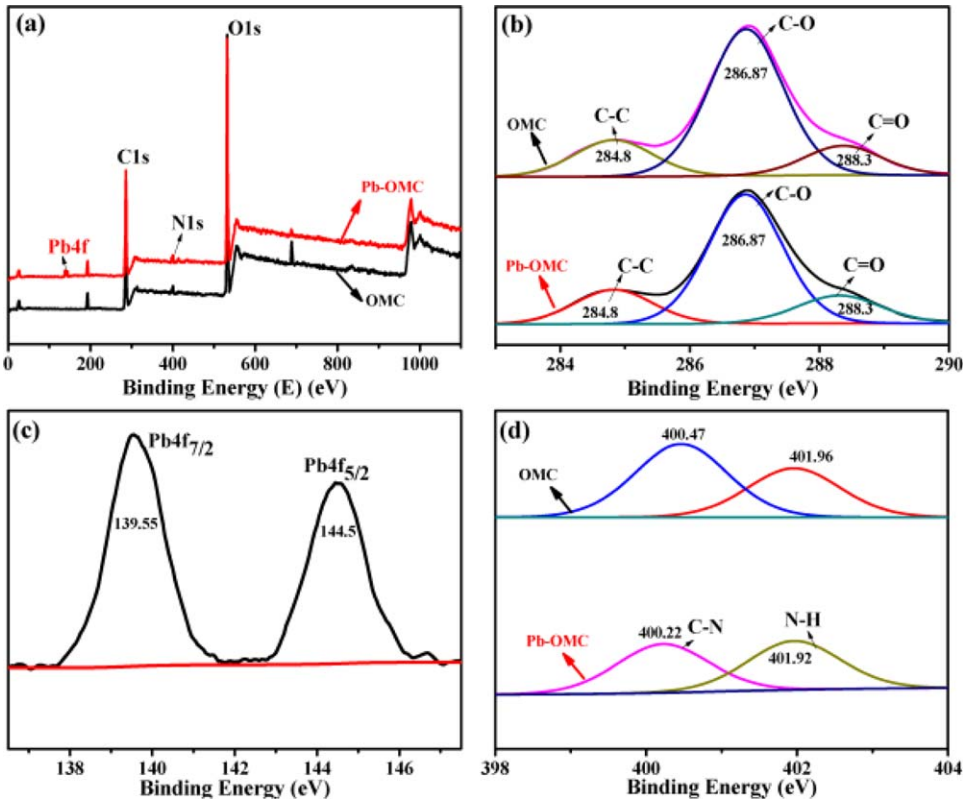

Figure 6. (a) XPS data survey of OMC and Pb-OMC; (b) High resolution C1sspectra; (c) High resolution Pb4f spectra; (d) High resolution N1s spectra. [Color figure can be viewed in the online issue, which is available at wileyonlinelibrary.com.]

obviously higher than that in this work (100 ppm). The above comparison further indicates the superior adsorption performance of OMC toward Pb(II) ions owing to the strong chelating interactions of Pb(II) with oxoacetohydrazide.

Reusability. The reusability of the OMC was evaluated. For each adsorption cycle, the used OMC was regenerated with 1M HCl to elute the adsorbed Pb(II). The regenerated OMC was then washed with excess water and dried in air for next adsorption cycle. Figure 5 shows the adsorption and elution efficiencies during three consecutive adsorption cycles. It reveals that the elution efficiencies obtained from all cycles were close to 100%. More importantly, over 95% of original adsorption capacity could be maintained after three cycles, indicating a superior reusability of OMC.

Mechanistic Aspects. The origin of the superior Pb(II) adsorption capability of OMC was investigated. The XPS spectra of OMC before and after Pb(II) adsorption were obtained [Figure 6(a)] and used to identify the interactions of the adsorbed Pb(II) with OMC. The high resolution spectra of C1s [Figure 6(b)] and N1s [Figure 6(d)] obtained from the as-synthesized OMC reveal non-oxygenated ring C (284.8 eV), C—O (286.87 eV), carbonyl C (288.3 eV), C—N (400.47 eV), and —NH (401.96 eV),[41] confirming a considerable number of oxoacetohydrazides being modified onto the cellulose. The high-resolution C1s spectrum obtained from the OMC with adsorbed Pb(II) is almost identical to that of the as-synthesized OMC, implying that the adsorbed Pb(II) is not directly interacted with those rings C, C—O, carbonyl C, and carbon in C—N. The XPS spectra of Pb4f [Figure 6(c)] reveal two peaks at 139.55 eV and 144.5 eV, corresponding to $Pb4f_{7/2}$ and $Pb4f_{5/2}$, respectively. The $Pb4f_{7/2}$ obtained from the adsorbed Pb(II)ions (139.55 eV) is 1.05 eV higher than that of free Pb(II) (138.50 eV),[42] confirming a strong interaction of the adsorbed Pb(II) with OMC. Such a strong binding energy shift suggests that the Pb(II) adsorption on OMC is through strong chemical interactions rather the weak physical interactions. The high resolution N1s spectra of OMC with and without adsorbed Pb(II)are shown in Figure 6(d). Comparing to the OMC without adsorbed Pb(II), the C—N and N—H binding energies of OMC with adsorbed Pb(II) are shifted from 400.47 to 400.27 eV and 401.96 to 401.92 eV, respectively. These binding energies shifts further suggest that the Pb(II) adsorption on OMC is via chemical interactions. Considering that the C—N and N—H are corresponding to —CONH— and $—NH_2$ groups, it can therefore be reasonably confident to suggest that the adsorption of Pb(II) on OMC is via the chelating interactions with the oxoacetohydrazide to form N—Pb—N bonds as illustrated in Scheme 2.

CONCLUSIONS

We have demonstrated a simple and environmental friendly oxoacetohydrazide functionalization method capable of converting the CC into high performance OMC adsorbents for effective Pb(II) removal. The resultant OMC possesses a dramatically improved Pb(II) adsorption capacity, over six times of the unmodified cellulose. The origin of the superior Pb(II)

adsorption capability of OMC can be attributed to the formation of N—Pb—N bonds resulting from the strong chelating interactions of Pb(II) with oxoacetohydrazide. Also, the OMC shows an excellent re-usability, capable of retain 95% of its original Pb(II) adsorption capacity after three consecutive adsorption cycles. The findings of this work pave a way to transform the agricultural by-products into high performance functional materials.

ACKNOWLEDGMENTS

This work was supported by the National Basic Research Program of China (Grant No. 2013CB934302), the Natural Science Foundation of China (Grant No. 51432009 and 21177132), and Strategic Priority Research Program of the Chinese Academy of Sciences (Grant No. XDA09030200).

REFERENCES

1. Kargarzadeh, H.; Sheltami, R. M.; Ahmad, I.; Abdullah, I.; Dufresne, A. *Polymer* **2015**, *56*, 346.
2. Wrigstedt, P.; Kylli, P.; Pitkänen, L.; Nousiainen, P.; Tenkanen, M.; Sipilä, J. *J Agric. Food Chem.* **2010**, *58*, 6937.
3. Majoinen, J.; Haataja, J. S.; Appelhans, D.; Lederer, A.; Olszewska, A.; Seitsonen, J.; Aseyev, V.; Kontturi, E.; Rosilo, H.; Österberg, M.; Houbenov, N.; Ikkala, O. *J Am. Chem. Soc.* **2013**, *136*, 866.
4. Ivanova, A.; Fattakhova-Rohlfing, D.; Kayaalp, B. E.; Rathouský, J.; Bein, T. *J Am. Chem. Soc.* **2014**, *136*, 5930.
5. Spinella, S.; Re, G. L.; Liu, B.; Dorgan, J.; Habibi, Y.; Leclère, P.; Raquez, J. M.; Dubois, P.; Gross, R. A. *Polymer* **2015**, *65*, 9.
6. Klemm, D.; Heublein, B.; Fink, H. P.; Bohn, A. *Angew. Chem. Int. Ed.* **2005**, *44*, 3358.
7. Wang, X.; Yang, K.; Tao, S.; Xing, B. *Environ. Sci. Technol.* **2006**, *41*, 185.
8. Habibi, Y.; Lucia, L. A.; Rojas, O. *J. Chem. Rev.* **2010**, *110*, 3479.
9. Gebald, C.; Wurzbacher, J. A.; Borgschulte, A.; Zimmermann, T.; Steinfeld, A. *Environ. Sci. Technol.* **2014**, *48*, 2497.
10. Batmaz, R.; Mohammed, N.; Zaman, M.; Minhas, G.; Berry, R. M.; Tam, K. C. *Cellulose* **2014**, *21*, 1655.
11. Low, K. S.; Lee, C. K.; Mak, S. M. *Wood Sci. Technol.* **2004**, *38*, 629.
12. Casarano, R.; Pires, P. A. R.; Borin, A. C.; Seoud, O. A. E. *Ind. Crop. Prod.* **2014**, *54*, 185.
13. Ong, R. C.; Chung, T. S.; Helmer, B. J.; Wit, J. S. *Polymer* **2013**, *54*, 4560.
14. Júnior, O. K.; Gurgel, L. V. A.; de Freitas, R. P.; Gil, L. F. *Carbohydr. Polym.* **2009**, *77*, 643.
15. Gurgel, L. V. A.; Gil, L. F. *Carbohydr. Polym.* **2009**, *77*, 142.
16. Ding, Z.; Yu, R.; Hu, X.; Chen, Y.; Zhang, Y. *Cellulose* **2014**, *21*, 1459.
17. Kono, H. *Carbohydr. Polym.* **2014**, *106*, 84.
18. Aoki, N.; Fukushima, K.; Kurakata, H.; Sakamoto, M.; Furuhata, K. *React. Funct. Polym.* **1999**, *42*, 223.
19. Zhao, B. X.; Wang, P.; Zheng, T.; Chen, C. Y.; Shu, J. *J. Appl. Polym. Sci.* **2006**, *99*, 2951.
20. Monier, M.; Nawar, N.; Abdel-Latif, D. A. *J. Hazard. Mater.* **2010**, *184*, 118.
21. Wang, X.; Zhao, J.; Guo, C.; Pei, M.; Zhang, G. *Sens. Actuator B-Chem.* **2014**, *193*, 157.
22. Neupane, L. N.; Park, J. Y.; Park, J. H.; Lee, K. H. *Org. Lett.* **2013**, *15*, 254.
23. Kim, H. N.; Ren, W. X.; Kim, J. S.; Yoon, J. *Chem. Soc. Rev.* **2012**, *41*, 3210.
24. Chen, W. S.; Yu, H. P.; Li, Q.; Liu, Y. X.; Li, J. *Soft Matter* **2011**, *7*, 10360.
25. Jiang, M.; Wang, J.; Li, L.; Pan, K.; Cao, B. *RSC Adv.* **2013**, *3*, 20625.
26. Yang, R.; Yu, S.; Aubrecht, K. B.; Wang, X.; Ma, H. Y.; Grubbs, R. B.; Hsiao, B. S.; Chu, B. *Polymer* **2015**, *60*, 9.
27. Halonen, H.; Larsson, P.; Iversen, T. *Cellulose* **2013**, *20*, 57.
28. Li, W. Y.; Jin, A. X.; Liu, C. F.; Sun, R. C.; Zhang, A. P.; Kennedy, J. F. *Carbohydr. Polym.* **2009**, *78*, 389.
29. Küçükgüzel, ŞG.; Oruç, E. E.; Rollas, S.; Şahin, F.; Özbek, A. *Eur. J. Med. Chem.* **2002**, *37*, 197.
30. Sedghi, R.; Heidari, B.; Behbahani, M. *J Hazard. Mater.* **2015**, *285*, 109.
31. Yang, R.; Aubrecht, K. B.; Ma, H.; Wang, R.; Grubbs, R. B.; Hsiao, B. S.; Chu, B. *Polymer* **2014**, *55*, 1167.
32. Amin, N. K. *Desalination* **2008**, *223*, 152.
33. Ho, Y. S.; McKay, G. *Water Res.* **1999**, *33*, 578.
34. Ho, Y. S.; McKay, G. *Process Biochem.* **1999**, *34*, 451.
35. Zhou, D.; Zhang, L.; Zhou, J.; Guo, S. *Water Res.* **2004**, *38*, 2643.
36. Shen, W.; Chen, S.; Shi, S.; Li, X.; Zhang, X.; Hu, W.; Wang, H. *Carbohydr. Polym.* **2009**, *75*, 110.
37. Musyoka, S. M.; Ngila, J. C.; Moodley, B.; Petrik, L.; Kindness, A. *Anal. Lett.* **2011**, *44*, 1925.
38. Wang, J.; Wei, L.; Ma, Y.; Li, K.; Li, M.; Ma, N.; Feng, K.; Wang, Y. *Desalin. Water Treat.* **2015**, *53*, 1641.
39. Chen, S.; Shen, W.; Yu, F.; Hu, W.; Wang, H. *J. Appl. Polym. Sci.* **2010**, *117*, 8.
40. Chen, S.; Zhou, Y.; Yan, Z.; Shen, W.; Shi, S.; Zhang, X.; Wang, H. *J. Hazard. Mater.* **2009**, *161*, 1355.
41. Kara, A.; Uzun, L.; Besirli, N.; Denizli, A. *J. Hazard. Mater.* **2004**, *106*, 93.
42. Wang, H.; Zhou, A.; Peng, F.; Yu, H.; Yang, J. *J. Colloid Interface Sci.* **2007**, *316*, 277.